Eur Radiol (2013) 23:887–896
DOI 10.1007/s00330-012-2691-z

GASTROINTESTINAL

Hepatocellular carcinoma in cirrhotic patients: prospective comparison of US, CT and MR imaging

Michele Di Martino · Gianmaria De Filippis · Adriano De Santis · Daniel Geiger · Maurizio Del Monte · Concetta Valentina Lombardo · Massimo Rossi · Stefano Ginanni Corradini · Gianluca Mennini · Carlo Catalano

Received: 25 April 2012 / Revised: 13 September 2012 / Accepted: 20 September 2012 / Published online: 18 November 2012

Abstract
Objectives To prospectively compare the diagnostic performance of ultrasound (US), multidetector computed tomography (MDCT) and contrast-enhanced magnetic resonance imaging (MRI) in cirrhotic patients who were candidates for liver transplantation.
Methods One hundred and forty consecutive patients with 163 hepatocellular carcinoma (HCC) nodules underwent US, MRI and MDCT. Diagnosis of HCC was based on pathological findings or substantial growth at 12-month follow-up. Four different image datasets were evaluated: US, MDCT, MRI unenhanced and dynamic phases, MRI unenhanced dynamic and hepatobiliary phase. Diagnostic accuracy, sensitivity, specificity, PPV and NPV, with corresponding 95 % confidence intervals, were determined. Statistical analysis was performed for all lesions and for three lesion subgroups (<1 cm, 1-2 cm, >2 cm).
Results Significantly higher diagnostic accuracy, sensitivity and NPV was achieved on dynamic + hepatobiliary phase MRI compared with US, MDCT and dynamic phase MRI alone. The specificity and PPV of US was significantly lower than that of MDCT, dynamic phase MRI and dynamic + hepatobiliary phase MRI. Similar results were obtained for all sub-group analyses, with particular benefit for the diagnosis of smaller lesions between 1 and 2 cm.
Conclusions Dynamic + hepatobiliary phase MRI improved detection and characterisation of HCC in cirrhotic patients. The greatest benefit is for diagnosing lesions between 1 and 2 cm.
Key Points
- *US, CT and MRI can all identify HCC in cirrhotic patients*
- *US has good sensitivity but suffers from false-positive findings*
- *Dynamic CT and MR have similar diagnostic performance for diagnosing HCC*
- *Dynamic + hepatobiliary phase MRI significantly improves detection and characterisation of HCC*
- *The greatest benefit is for the diagnosis of lesions between 1 and 2 cm*

Keywords Hepatocellular carcinoma · Ultrasound · Multidetector computed tomography · Magnetic resonance imaging · Liver specific contrast agent

M. Di Martino · G. De Filippis · D. Geiger · M. Del Monte · C. V. Lombardo · C. Catalano (✉)
Department of Radiological Sciences, Oncology and Anatomical Pathology, University of Rome "Sapienza",
Viale Regina Elena 324,
Rome 00161, Italy
e-mail: carlo.catalano@uniroma1.it

A. De Santis · S. G. Corradini
Department of Clinical Medicine, Division of Gastroenterology, University of Rome "Sapienza",
Viale Regina Elena 324,
Rome 00161, Italy

M. Rossi · G. Mennini
Department of General Surgery, Division of Organ Transplantation, University of Rome "Sapienza",
Viale Regina Elena 324,
Rome 00161, Italy

Introduction

Hepatocellullar carcinoma (HCC) is the fifth most common cancer worldwide and the third leading cause of cancer-related death [1, 2]. It occurs primarily in subjects who have chronic liver disease or liver cirrhosis and is the primary cause of death among this group. Some centres advocate use of ultrasound (US) and α-fetoprotein (AFP) in a 6-month periodical screening program, while other associations such as UNOS (United

Network for Organ Sharing) have policies that support the use of contrast-enhanced magnetic resonance imaging (MRI) or multidetector-row computed tomography (MDCT) over US. Among cirrhotic patients suspected of having developed HCC, non-invasive diagnostic imaging using either MRI or MDCT is frequently the management approach utilised for the detection and characterisation of lesions, and subsequently for tumour staging and treatment planning.

Unfortunately, despite numerous technological developments and improvements in recent years, the diagnostic accuracy of non-invasive imaging in patients with cirrhosis is still relatively low, ranging respectively between 0.60 and 0.72 for US, between 0.74 and 0.83 for MDCT and between 0.71 and 0.87 for MRI [3–17]. The introduction of the cellular specific MRI contrast agents has also been demonstrated to be able to significantly increase the detection of HCC in cirrhotic patients compared with MDCT, with a diagnostic accuracy ranging between 0.88 and 0.95 [17–21]. The relatively poor diagnostic performance for the detection of HCC in cirrhotic liver is due principally to overlapping imaging features and, thus, difficulties in differentiating dysplastic nodules from small HCC, and to problems associated with diagnosing arterially enhancing nodules smaller than 2 cm in diameter. For these reasons patients generally undergo regular follow-up with CT or MRI.

The aim of this study was to prospectively compare the diagnostic performance of state-of-the-art US, MDCT and contrast-enhanced MRI in a population of cirrhotic patients who were candidates for liver transplantation.

Materials and methods

Study population

This study was approved by our institutional review board and followed the principles of the Declaration of Helsinki and subsequent amendments. All patients provided written informed consent.

Between January 2007 and July 2010, 250 consecutive patients with chronic liver disease were evaluated prospectively within the Liver Transplant Unit of the Department of Gastroenterology regarding the possibility for liver transplantation. Patients were eligible for this study if they underwent imaging with US, MDCT and MRI within 1 month and had histologically proven cirrhosis at liver biopsy. Patients were ineligible and were excluded from the study if they were younger than 18 years of age, were pregnant or lactating females, were contraindicated for MRI (e.g. because of pacemaker, ferromagnetic clips, claustrophobia), had a previous history of anaphylactoid reaction to iodinated contrast agents or had severe renal impairment (glomerular filtration rate or estimated glomerular filtration rate <30 ml/min/1.73 m^2).

Of the 250 evaluated patients, 60 were not considered suitable for liver transplant surgery and were excluded (history of previous neoplasia, n=6; severe cardiopulmonary disease, n=20; end-stage liver disease, n=5; diffuse metastatic disease, n=16; active drug/alcohol abuse, n=13).

Of the remaining 190 patients 15 did not undergo MRI (claustrophobia, n=4; pacemaker, n=3; ferromagnetic clips, n=2; non-diagnostic MRI exam due to inability to suspend respiration, n=6), 10 were lost to imaging follow-up, 22 failed to undergo all three imaging examinations within 30 days, 3 were excluded because at histological examinations reported 3 cholangiocarcinoma nodules (two patients) and 3 hepatocholangiocarcinoma nodules (one patient). The final study population therefore comprised 140 patients (mean age, 59 years; range, 23–82 years) of which 104 were male (mean age, 66 years; range, 35–80 years) and 36 female (mean age, 55 years; range, 23–82 years). Overall, 71 patients were classified as Child-Pugh A, 43 as Child-Pugh B and 26 as Child-Pugh C.

All patients underwent US for the first examination. Thereafter, 93 patients underwent MDCT followed by MRI (mean interval, 20 days; range 1–30 days) while 47 patients underwent MRI followed by CT (mean interval, 19 days; range, 1–30 days).

US

US examinations (Sonoline Antares; Siemens, Erlangen, Germany) were performed using a curved array or sector probe with a centre frequency of 2–5 MHz. A higher-frequency linear-array probe was also used to better evaluate the liver surface. Evaluations of subxyphoid, subcostal and intercostal regions were performed during quiet respiration and during end-expiration breath-hold. The subcostal approach was performed with the patient in the left lateral decubitus position in deep inspiration allowing insonation of the majority of the right lobe, including the dome. Liver lesions were assessed for echogenicity and homogeneity. Lesion vascularity was assessed using power-colour Doppler US with spectral analysis of intratumoral and peritumoral vessels.

MDCT

Multiphasic CT was performed in the cranio-caudal direction using 64-slice MDCT (Somatom Sensation 64; Siemens Medical Systems, Erlangen, Germany) with detector configuration 64 (32×2)×0.6; tube voltage, 120 kVp; tube current, 250 mAs; gantry rotation time, 0.33 s; pitch, 1; CT data acquisition time, 4–11 s; slice thickness in the axial and coronal planes, 5 mm (unenhanced) or 3 mm (enhanced)

with no interslice gap. A soft tissue B20 kernel was used in all cases. All patients received 1.4 ml/kg bodyweight (corresponding to 560 mg iodine/kg) of Iomeprol-400 (Iomeron 400; Bracco Imaging, Milan, Italy), a non-ionic contrast medium (CM) formulated to contain a high concentration of iodine (400 mg/ml). Pre-warmed CM was administered intravenously using a dual-chamber mechanical power injector (Stellant D CT; Medrad, Indianola, PA, USA) at a rate of 4 ml/s through an 18-gauge IV catheter inserted into an antecubital vein. All injections were followed by a 30 ml saline flush administered at the same injection rate. After acquisition of an anteroposterior digital scout radiograph, patients were scanned craniocaudally from the dome of the liver to the iliac crest before and after intravenous contrast medium administration. Images were obtained during the hepatic arterial, hepatic venous and delayed phases (25–40, 70, and 180 s, respectively, after the start of contrast medium injection).

The delay before initiation of the hepatic arterial phase CT data acquisition was determined by means of bolus-tracking with automated triggering (CARE Bolus CT; Siemens Medical Systems, Erlangen, Germany). Arterial phase CT data acquisition began automatically 18 s after a trigger threshold of 150 Hounsfield units (HU) was reached in the supra-coeliac abdominal aorta.

MRI

MRI was performed in all patients at 1.5 T (Magnetom Avanto; Siemens Medical Systems), equipped with a 32-channel system, a maximum gradient strength of 45 mT/m and a peak slew rate of 200 mT/m/ms. Images were acquired in the transverse plane during end-expiratory breath-hold using a combined six-channel anteroposterior phased-array surface coil and a spine-array coil. MRI sequences and parameters are detailed in Table 1 Parallel imaging with an IPAT factor 2 was applied in conjunction with a three-quarter field of view in the phase encoding direction. The overall acquisition time was approximately 18 s.

The MR contrast agent used was gadobenate dimeglumine (MultiHance; Bracco Imaging, Milan, Italy), which was administered at 0.2 ml/kg bodyweight, corresponding to a dose of 0.1 mmol/kg bodyweight. All injections were performed by power injector at a rate of 2 ml/s through an antecubital vein and were flushed with 20 ml saline administered at the same rate.

To determine the optimal timing for the hepatic arterial phase, a fluoroscopic bolus detection technique was used in all patients. The arterial phase began 8 s after contrast arrival at the supraceliac abdominal aorta. The enhanced images were acquired during the arterial, portal-venous and delayed phases at approximately 22–35 s, 70 s and 180 s after gadobenate dimeglumine administration, respectively: the hepatobiliary phase was also achieved after 90 min.

Standard of reference

A composite reference standard was used to diagnose or rule out HCC. A diagnosis of HCC required one or more of the following criteria: histological confirmation (liver biopsy, resection and transplantation) or demonstration of substantial growth at a minimum imaging follow-up of 12 months, defined as an increase in the longest lesion diameter of >5 mm at either CT or MRI [22].

All resected and explanted livers were analysed by the same experienced (>25 years) pathologist; they were sectioned in the axial plane with a slice thickness of 5–10 mm. The preoperative CT and MRI findings were directly correlated with histological findings by an expert radiologist with 5 years' experience in abdominal imaging who was present when the specimens were prepared for evaluation.

All lesions detected at diagnostic imaging were analysed histologically; if a lesion was not macroscopically visible, the area of liver parenchyma as close as possible to the abnormality detected at imaging was selected for histological analysis. Moreover, every zone of parenchyma that differed from the surrounding liver in colour, texture or morphology was analysed. All lesions were classified according to accepted guidelines [23].

Table 1 MRI sequences and parameters

MR sequence	Fat suppression	Intravenous contrast medium	Repetition time/echo time	Flip angle	Section thickness	Matrix size
T2-weighted 2D TSE	Not used	Unenhanced images	4,000/176 ms	150°	5 mm	192×256
T1-weighted 2D GRE	Not used	Unenhanced images	140/2.2–4.4 ms	90°	5 mm	192×256
T1-weighted 3D spoiled GRE VIBE[a]	Used	Unenhanced and enhanced images	5.7/2.8 ms	10°	3 mm	192×256

GRE gradient echo, *TSE* turbo spin echo, *VIBE* volumetric interpolated breath-hold examination

[a] Images were acquired 25–40, 70 and 180 s after contrast medium injection during hepatic arterial, portal-venous, delayed phases, and after 90 min during the hepatobiliary phase

Percutaneous needle nodule biopsy was performed with an 18-gauge needle, under local anaesthesia and US guidance. Each biopsy specimen was approximately 1.5 cm in length.

Image analysis

Four different image datasets were evaluated: (1) US, (2) MDCT, (3) MRI unenhanced + enhanced dynamic phase, (4) MRI unenhanced + enhanced dynamic phase + enhanced hepatobiliary phase.

US examinations were archived as real-time movies and evaluated on site, in consensus, by two experienced gastrointestinal clinicians (A.D.S., S.G.C.; with 28 and 10 years' experience in US imaging of the liver, respectively). CT and MRI datasets were evaluated, at the time of the examinations, on a commercially available workstation by two further experienced gastrointestinal radiologists (C.C. and M.D.M.; with 22 and 10 years' experience in both CT and MRI of the liver, respectively). Disagreement between readers was resolved by a third observer (G.D.F.), whose decision was considered for statistical analysis.

To minimise any recall bias, each reading session was separated by an interval of at least 4 weeks.

Readers were aware of the imaging phase and that all patients had cirrhosis, but they were unaware of the results of other imaging exams, and AFP levels and were blinded to all other patient radiological and clinical information.

Detected lesions were characterised as HCC if the appearance on diagnostic imaging met certain specific criteria determined before the start of the study [9, 21, 24–26].

US criteria: Lesions that were hypoechoic, heterogeneously hyperechoic or echoic with a peripheral hypoechoic rim were considered HCC. High-velocity systolic and diastolic signals at power-colour Doppler US were also considered indicative of malignancy. Lesions that did not demonstrate these features were considered benign.

CT criteria: Lesions that demonstrated enhancement during the arterial phase and contrast wash-out during the portal-venous and/or delayed phases were considered HCC. Indicative but non-conclusive features for HCC also included arterial enhancement or hypoattenuation compared with the surrounding liver parenchyma, with or without peripheral rim enhancement (fibrous capsule), in the delayed phase.

MRI criteria: Lesions that demonstrated enhancement during the arterial phase, wash-out during the delayed and/or hepatobiliary phases, and peripheral rim enhancement during the delayed phase were considered HCC. Suggestive but non-conclusive criteria for HCC were mild hyperintensity on T2-weighted images or nodular early enhancement without contrast wash-out.

Each detected lesion was assessed for confidence in characterisation using a four-point scale in which 1 = benign, 2 = probably benign, 3 = probably malignant, 4 = malignant. Lesions ascribed a confidence score of 3 or 4 were considered malignant while lesions ascribed a score of 1 or 2 were considered benign.

Moreover all lesions were also divided, according to their size, into three groups (>2 cm, 1–2 cm and <1 cm).

Statistical analysis

The diagnostic performance of each imaging modality for the identification of HCC was determined for all lesions and for three subgroups of lesions based on lesion size (>2 cm, 1–2 cm, <1 cm). Determinations of the sensitivity, specificity, accuracy, and positive and negative predictive values (PPV and NPV, respectively) for lesion detection on each image set for each reader were calculated against composite reference standard findings. In each case lesions assigned a confidence score of 3 or 4 were considered true positive (TP) for malignancy if the reference standard findings indicated a malignant lesion. Conversely, lesions assigned a score of 1 or 2 were considered true negative (TN) if the reference standard findings indicated a benign lesion. Lesions assigned a confidence score of 3 or 4 were considered false positive (FP) for malignancy if the reference standard findings indicated a benign lesion. Lesions assigned a confidence score of 1–2 were considered false negative (FN) if the reference standard findings indicated a malignant lesion. The 95 % confidence interval (CI) was determined for each evaluation.

To account for the presence of clustered data (i.e. several nodules in a single patient), the accuracy of each imaging method was determined using Jackknife Alternative Free-response Receiver Operating Characteristic (JAFROC) analysis (JAFROC, version 2.1; downloaded from http://www.devchakraborty.com) [27]. The area under the alternative free-response receiver operating characteristic curve A_1 (AUC) was used to assess the overall diagnostic performance of each reader on each image set.

A modified adjusted χ^2 test was used to test for differences in sensitivity, specificity, PPV and NPV between MRI and MDCT, taking into account correlations between multiple lesions within the same patient [28].

Results

A total of 254 confirmed lesions comprising 163 diagnosed HCC nodules and 91 benign lesions were present in 106 of the 140 patients in our population. In the remaining 34 patients no lesions were identified either at initial imaging or at follow-up after a minimum of 12 months.

Sixteen out of the 34 patients with no lesions underwent liver transplantation.

The 163 HCC nodules (mean size 2.3±2.4 cm, range 0.4–17 cm) were present in 77/140 (55 %) patients. Of these 163 lesions, 99, in 50 patients, were confirmed histologically (77 lesions in 32 patients who underwent liver transplantation, 6 lesions in 6 patients who underwent surgery, 16 lesions in 12 patients who underwent biopsy), whereas 64 lesions in 27 patients were confirmed at follow-up imaging after a minimum of 12 months.

Of the 91 benign lesions, 51 (mean size, 2.1±0.9 cm; range, 0.5–6 cm) were found in 29 patients (20 %) with no malignant lesions and comprised 13 regenerative nodules, 5 dysplastic nodules, 6 hemangiomas, 4 areas of confluent fibrosis, 17 arterial-venous shunts, 3 siderotic nodules, 2 areas of necrosis, one leiomyoma. The remaining 40 benign lesions (mean size, 1.4±0.8 cm; range, 0.5–4.4 cm) comprised 24 regenerative nodules, 7 dysplastic nodules, 5 hemangiomas, 3 areas of necrosis and 1 area of confluent fibrosis, and were present in 20 patients who also presented concomitant malignant lesions. These 91 benign lesions were confirmed either histologically (44 lesions, comprising 33 lesions in 19 patients who underwent liver transplantation, 7 lesions in 5 patients who underwent biopsy and 4 lesions in 2 patients who underwent hepatectomy) or at subsequent imaging follow-up (47 lesions in 23 patients).

Diagnostic performance

Regardless of lesion size, more malignant lesions were detected on MRI datasets that included unenhanced, dynamic and hepatobiliary phase images than were detected on US or MDCT datasets or MRI datasets that included only unenhanced and dynamic phase images (Table 2). Specifically, the sensitivity for malignant lesion detection was significantly higher for all lesions detected ($P<0.001$; for all comparisons) and for lesions between 1 and 2 cm in size ($P=0.03$ vs US; $P=0.007$ vs MDCT and $P=0.005$ dynamic phase MRI alone). All lesions larger than 2 cm in size (58/58) were detected on dynamic + hepatobiliary phase MRI and most were also detected on US, MDCT and dynamic phase MRI alone. Similar findings were obtained regarding

Table 2 Diagnostic performance for detection of HCC with US, MDCT and MRI

Lesion population	Parameter	US	MDCT	MRI (pre + dynamic phases)	MRI (pre + dynamic + hepatobiliary phases)
All lesions	Sensitivity	0.71 (117/163)	0.71 (117/163)	0.71 (117/163)	0.87 (142/163) [a]
		[0.64, 0.78]	[0.64, 0.78]	[0.64, 0.78]	[0.81, 0.92]
	Specificity	0.62 (57/91) [b]	0.87 (79/91)	0.87 (79/91)	0.90 (83/91)
		[0.50, 0.68]	[0.78, 0.93]	[0.78, 0.96]	[0.81, 0.96]
>2 cm	Sensitivity	0.93 (54/58)	0.93 (54/58)	0.95 (55/58)	1.0 (58/58)
		[0.83, 0.98]	[0.83, 0.98]	[0.86, 0.99]	[0.94, 1.0]
	Specificity	0.46 (16/30) [c]	0.90 (27/30)	0.87 (26/30)	0.93 (28/30)
		[0.22, 0.59]	[0.73, 0.97]	[0.69, 0.96]	[0.78, 0.99]
1–2 cm	Sensitivity	0.70 (58/83)	0.65 (54/83)	0.66 (55/83)	0.85 (71/83) [d]
		[0.59, 0.79]	[0.54, 0.75]	[0.55, 0.76]	[0.76, 0.92]
	Specificity	0.60 (28/47) [e]	0.89 (42/47)	0.91 (43/47)	0.94 (44/47)
		[0.44, 0.73]	[0.77, 0.96]	[0.80, 0.98]	[0.82, 0.99]
<1 cm	Sensitivity	0.22 (5/22)	0.36 (8/22)	0.36 (8/22)	0.59 (13/22)
		[0.06, 0.45]	[0.17, 0.59]	[0.17, 0.59]	[0.36, 0.79]
	Specificity	0.93 (13/14)	0.71 (10/14)	0.71 (10/14)	0.78 (11/14)
		[0.66, 0.99]	[0.42, 0.92]	[0.42, 0.92]	[0.63, 0.80]

Numbers in square brackets are 95 % confidence intervals

[a] Significantly higher sensitivity on dynamic + hepatobiliary phase MRI compared with US, MDCT and dynamic phase MRI alone ($P<0.001$; all comparisons)

[b] Significantly lower specificity on US compared with MDCT, dynamic phase MRI alone and dynamic + hepatobiliary phase MRI ($P<0.001$)

[c] Significantly lower specificity on US compared with MDCT ($p<0.001$), dynamic phase MRI alone ($P=0.002$); dynamic + hepatobiliary phase MRI ($P<0.001$)

[d] Significantly higher sensitivity on dynamic + hepatobiliary phase MRI compared with US ($P=0.03$), MDCT ($P=0.007$) and dynamic phase MRI alone ($P=0.005$)

[e] Significantly lower specificity on US compared with MDCT ($P=0.002$), dynamic phase MRI alone ($P<0.001$); dynamic + hepatobiliary phase MRI ($P<0.001$)

Table 3 Diagnostic accuracy for detection of HCC with US, MDCT and MRI determined using JAFROC analysis

Lesion population	US	MDCT	MRI (pre + dynamic phases)	MRI (pre + dynamic + hepatobiliary phases)
All lesions	0.72 [0.66, 0.77] [d]	0.80 [0.75, 0.85]	0.83 [0.80, 0.89]	0.90 [0.85, 0.93] [a]
>2 cm	0.70 [0.59, 0.79] [e]	0.90 [0.82, 0.95]	0.90 [0.81, 0.95]	0.97 [0.91, 0.99] [b]
1–2 cm	0.64 [0.55, 0.72] [f]	0.79 [0.70, 0.85]	0.84 [0.75, 0.89]	0.90 [0.83, 0.95] [c]
<1 cm	0.58 [0.40, 0.74]	0.57 [0.39, 0.73]	0.56 [0.38, 0.72]	0.62 [0.45, 0.73]

Numbers in square brackets are 95 % confidence intervals

[a] Significantly higher accuracy on dynamic + hepatobiliary phase MRI compared with US, MDCT and dynamic phase MRI alone ($P<0.001$; all comparisons)

[b] Significantly higher accuracy on dynamic + hepatobiliary phase MRI compared with US ($P<0.001$), MDCT ($P=0.015$) and dynamic phase MRI alone ($P=0.047$)

[c] Significantly higher accuracy on dynamic + hepatobiliary phase MRI compared with US, MDCT and dynamic phase MRI alone ($P<0.001$; all comparisons)

[d] Significantly lower accuracy on US compared with MDCT ($P\leq0.001$), dynamic phase MRI ($P=0.001$) and dynamic + hepatobiliary phases MRI ($P<0.001$)

[e] Significantly lower accuracy on US compared to MDCT ($P\leq0.001$), dynamic phase MRI ($P=0.001$) and dynamic + hepatobiliary phases MRI ($P<0.001$)

[f] Significantly lower accuracy on US compared with MDCT ($P=0.018$), dynamic phase MRI ($P=0.001$) and dynamic and hepatobiliary phase MRI ($P<0.001$)

the specificity for lesion detection. Significantly ($P\leq0.002$) better specificity for all lesions and for the two lesion subgroups larger than 1 cm was obtained for MRI datasets that included unenhanced, dynamic and hepatobiliary phase images than was obtained for US and MDCT datasets, and MRI datasets that included only unenhanced and dynamic phase images (Table 2).

The overall accuracy for the detection of HCC was significantly ($P\leq0.047$) higher on dynamic + hepatobiliary phase MRI compared with US, MDCT and dynamic MRI

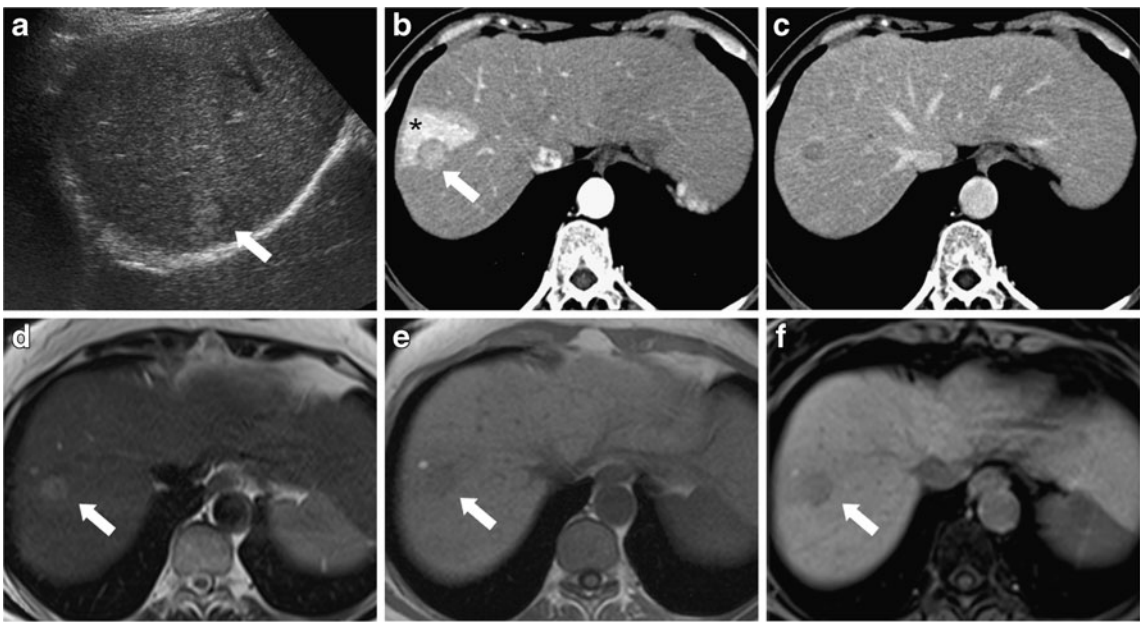

Fig. 1 A 60-year-old woman with Child-Pugh A hepatitis C cirrhosis who underwent liver transplantation. US (**a**) reveals a suspicious hyperechoic nodule in liver segment VIII with peripheral hypoechoic aloe (*arrow*). CTs acquired during the arterial (**b**) and delayed (**c**) phases show a hypervascular nodule with typical contrast wash-out (*arrow*). Note the presence of an area of transient hepatic attenuation defect ("THAD" lesion) (*). The T2-weighted MR image (**d**) reveals a nodule that is slightly hyperintense to the surrounding liver (*arrow*). On the fat-suppressed T1-weighted GRE unenhanced image (**e**) the lesion is slightly hypointense to the surrounding liver (*arrow*). The fat-suppressed T1-weighted 3D spoiled-GRE MR images obtained during the arterial and delayed phases show a lesion whose enhancement pattern is similar to that seen at CT. On the fat-suppressed T1-weighted 3D spoiled GRE image (**f**) acquired at the same level during the hepatobiliary phase (90 min after injection), the lesion is characteristically hypointense to the surrounding liver (*arrow*)

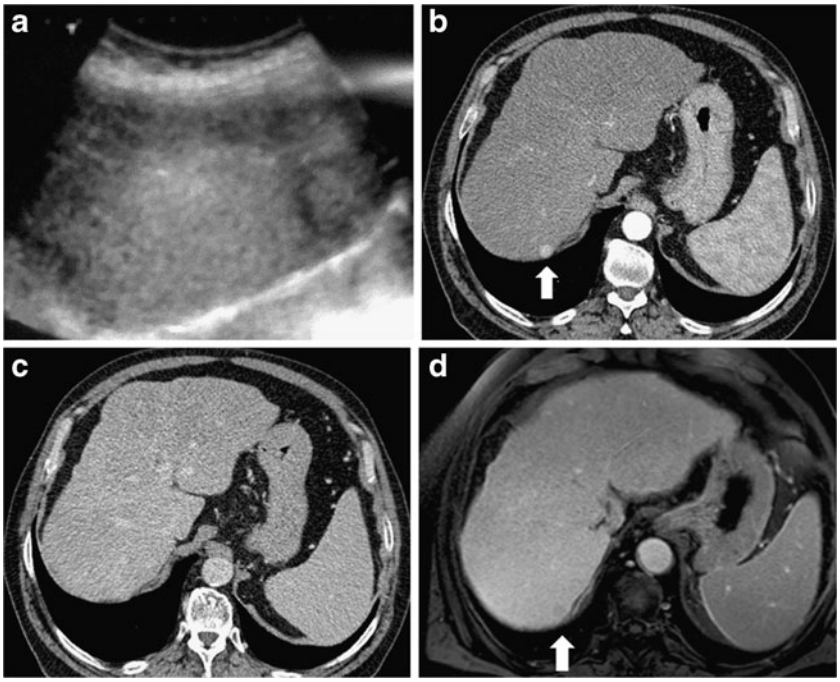

Fig. 2 A 68-year-old-man with Child-Pugh A alcoholic cirrhosis who underwent liver transplantation. The US image (**a**) does not reveal any focal liver lesion in liver segment VII. The CT contrast-enhanced axial image (**b**) obtained during the arterial phase reveals a tiny hypervascular round lesion (*arrow*) near the liver surface. The lesion is isoattenuating compared with the surrounding liver during the delayed phase (**c**). The corresponding fat-suppressed T1-weighted spoiled GRE image acquired during hepatic arterial and delayed phases reveals a lesion enhancement pattern similar to that seen at CT. On the fat-suppressed T1-weighted 3D spoiled GRE image (**d**) obtained during the hepatobiliary phase at 90 min after contrast injection the lesion is markedly hypointense, indicating that functioning hepatocytes are absent from the lesion and that, therefore, the lesion is malignant (*arrow*). This lesion was considered benign at both MDCT and dynamic phase MRI. The hepatobiliary phase image markedly increased the conspicuity of the lesion, enabling correct characterisation as HCC

alone for all lesions, and for the two lesion subgroups larger than 1 cm (Table 3). Using the same JAFROC analysis, the accuracy for detection of HCC on US image datasets was significantly lower than that on MDCT and both MRI image datasets for all lesions, and for lesion subgroups larger than 1 cm.

Overall, of the 163 confirmed HCC nodules, 93 (56 %) nodules were correctly identified on all image datasets (Fig. 1), whereas 14 (five 1–2 cm, nine <1 cm) that were all confirmed at liver transplantation were not identified on any dataset. A total of 142 nodules (87 %) were correctly identified on dynamic + hepatobiliary phase MRI. Of these 142 nodules, 128 (90.1 %) were hypointense on hepatobiliary phase images, whereas 14 (9.9 %) were isointense to hyperintense. Seven of these latter lesions were identified and correctly diagnosed because of characteristic vascular enhancement patterns during the dynamic phase. The 21 nodules not detected on dynamic + hepatobiliary phase MRI were predominantly small (12 1–2 cm, nine <1 cm) and were considered FN for determinations of diagnostic performance

Notably, only eight lesions were determined to be FP on dynamic + hepatobiliary phase MRI, compared with 12 on both MDCT and dynamic phase MRI, and 38 on US. The 38 FP findings at US included 20 hypoechoic lesions and 6 hyperechoic nodules that were confirmed as regenerative nodules, 9 further hyperechoic nodules that were confirmed as hemangiomas and 3 further hypoechoic lesions with peripheral hyperechoic halos that were confirmed as siderotic nodules. The 12 FP findings in 11 patients at MDCT included the same FP lesion detected at dynamic phase MRI plus 3 regenerative nodules, 6 arterial-venous shunts, 2 hemangiomas and 1 focal liver haemorrhage. Four of these 12 lesions were correctly characterised on dynamic + hepatobiliary phase MRI. Finally, the eight FP lesions (two >2 cm, three 1–2 cm, three <1 cm) on dynamic + hepatobiliary phase MRI were confirmed at histology to be five regenerative nodules (three 1–2 cm, two<1 cm), two dysplastic nodules (>2 cm) and one area of fibrosis (<1 cm).

Regarding the impact of hepatobiliary phase MRI, the availability of these images helped provide a definitive diagnosis of malignancy for 21/83 (25.3 %) nodules of 1–2 cm in diameter. Moreover, 10/83 (12.0 %) lesions that were not detected or were assigned a low confidence score at US, MDCT and dynamic phase MRI were correctly characterised as malignant only on hepatobiliary phase MR images (Fig. 2). Superiority for dynamic + hepatobiliary phase MRI was also noted for small (<1 cm) lesions,

although there were too few lesions of this size to demonstrate statistical significance.

Both the PPV and NPV for HCC identification were higher on dynamic + hepatobiliary phase MRI compared with US, MDCT and dynamic phase MRI alone (Table 4), indicating that the likelihood of identifying malignant nodules is greater and that the risk of overlooking malignant disease is lower if hepatobiliary phase images are acquired.

The PPV determined for US was significantly ($P \leq 0.005$) lower than that determined for MDCT and both MRI datasets. Likewise, a significantly higher ($P \leq 0.047$) NPV was noted for dynamic + hepatobiliary phase MRI for all size lesions and for lesions of 1–2 cm in diameter.

Discussion

Routine surveillance of cirrhotic patients is extremely important due to the high prevalence of HCC and to the fact that early detection and diagnosis of HCC nodules may allow potentially curative treatment strategies such as liver transplantation or surgery.

To our knowledge, few studies have prospectively compared the sensitivity, specificity and overall diagnostic accuracy of US, MDCT and gadobenate dimeglumine-enhanced MRI for the detection of HCC in a large population of patients with cirrhosis [7–9]. Our study, which was performed using state-of-the-art equipment and highly specialised personnel for each imaging investigation, revealed that of these four imaging techniques by far the most sensitive, specific and accurate was dynamic + hepatobiliary phase MRI enhanced with gadobenate dimeglumine. Conversely, US was significantly inferior to dynamic + hepatobiliary phase MRI in terms of diagnostic accuracy for all but the smallest nodules (<1 cm), of which there were comparatively few in the lesion population. Although the sensitivity of US for HCC detection was slightly higher than previously reported values [3, 4] and bore good comparison with values determined for MDCT and dynamic phase MRI alone, this technique suffered in terms of specificity, primarily because of a relatively high number of

Table 4 Predictive values for detection of HCC with US, MD CT and MRI

Lesion population	Parameter	US	MDCT	MRI (pre + dynamic phase)	MRI (pre + dynamic + hepatobiliary phases)
All lesions	PPV	0.71 (117/151) [a]	0.91 (117/129)	0.91 (117/129)	0.95 (142/150)
		[0.68, 0.82]	[0.75, 0.85]	[0.75, 0.85]	[0.90, 0.98]
	NPV	0.55 (57/103)	0.63 (79/125)	0.63 (79/125)	0.80 (83/104) [b]
		[0.43, 0.64]	[0.54, 0.71]	[0.54, 0.71]	[0.70, 0.87]
>2 cm	PPV	0.77 (54/70) [c]	0.95 (54/57)	0.93 (55/59)	0.97 (58/60)
		[0.63, 0.84]	[0.85, 0.98]	[0.83, 0.98]	[0.88, 0.99]
	NPV	0.77 (14/18)	0.87 (27/31)	0.89 (26/29)	1.0 (28/28)
		[0.48, 0.93]	[0.70, 0.96]	[0.73, 0.98]	[0.88, 1.0]
1–2 cm	PPV	0.75 (58/77) [d]	0.91 (54/59)	0.93 (55/59)	0.96 (71/74)
		[0.64, 0.84]	[0.81, 0.97]	[0.83, 0.98]	[0.88, 0.99]
	NPV	0.53 (28/53)	0.59 (42/71)	0.61 (43/71)	0.79 (44/56) [e]
		[0.39, 0.67]	[0.47, 0.71]	[0.48, 0.72]	[0.65, 0.88]
<1 cm	PPV	0.83 (5/6)	0.67 (8/12)	0.67 (8/12)	0.81 (13/16)
		[0.35, 0.99]	[0.35, 0.90]	[0.35, 0.90]	[0.54, 0.96]
	NPV	0.43 (13/30)	0.42 (10/24)	0.42 (10/24)	0.55 (11/20)
		[0.25, 0.62]	[0.22, 0.63]	[0.29, 0.68]	[0.31, 0.76]

Numbers in square brackets are 95 % confidence intervals

[a] Significantly lower PPV on US compared with MDCT, dynamic phase MRI alone ($P=0.005$); dynamic + hepatobiliary phase MRI datasets ($P<0.001$; all comparisons)

[b] Significantly higher NPV on dynamic + hepatobiliary phase MRI compared with US ($P<0.001$), MDCT and dynamic phase MRI alone ($P=0.007$)

[c] Significantly lower PPV on US compared with MDCT ($P=0.009$), dynamic phase MRI alone ($P=0.024$); dynamic + hepatobiliary phase MRI ($P=0.002$) datasets

[d] Significantly lower PPV on US compared with MDCT ($P=0.029$), dynamic phase MRI alone ($P=0.011$); dynamic + hepatobiliary phase MRI ($P<0.001$) datasets

[e] Significantly higher NPV on dynamic + hepatobiliary phase MRI compared with US ($P=0.007$), MDCT ($P=0.02$) and dynamic phase MRI alone ($P=0.047$)

FP interpretations. As regards MDCT and dynamic phase MRI alone, a slight albeit non-significant tendency for better overall diagnostic performance was noted for the latter technique, although the differences were too small for either technique to be considered superior to the other. Both techniques have previously been shown to be effective for the detection and characterisation of focal liver lesions in cirrhotic patients [5, 6].

As several studies have reported in the literature [10–14], this study—conducted in a cirrhotic study population—confirms that hepatobiliary phase MR images enabled improved diagnostic accuracy for the detection of HCC, primarily due to a reduced number of FP determinations. Despite recent guidelines that suggest a cut-off value of 1 cm for the non-invasive diagnosis of HCC [29], our results show that the sensitivity of conventional imaging techniques is still relatively poor, even for the identification of nodules between 1 and 2 cm in size. On the other hand, MRI with the additional availability of hepatobiliary phase images showed very promising results for the evaluation of nodules of this size (diagnostic accuracy, 0.90; sensitivity, 0.85; specificity, 0.94).

As regards lesions smaller than 1 cm, dynamic + hepatobiliary phase MRI was again the best method for identification, although the overall diagnostic performance (diagnostic accuracy, 0.62; sensitivity, 0.59; specificity, 0.78) was somewhat poorer than for larger lesions.

To note is that HCC may present different enhancement patterns on hepatobiliary phase images after gadobenate dimeglumine administration, depending on the degree of differentiation of the HCC nodule and the extent of its residual capacity to take up the Gd-BOPTA contrast-effective molecule of gadobenate dimeglumine [30]. Thus, certain HCC nodules retain a certain degree of residual functionality and appear isointense or hyperintense on hepatobiliary phase images, whereas other HCC nodules that have lost all functionality appear hypointense [31–33]. In our study most HCC nodules appeared hypointense. Of the 14 nodules that appeared isointense or hyperintense on delayed hepatobiliary phase images, seven were successfully characterised as HCC based on their enhancement pattern on dynamic phase images.

Our study shows that of the routine non-invasive approaches to diagnosing HCC in patients with cirrhosis, by far the most sensitive and accurate diagnostic performance is achieved on MRI enhanced with a hepatobiliary contrast agent.

Six lesions in three patients (excluded from the study population), turned out to be at histology not HCC (three mixed tumours, three cholangiocarcinomas); at imaging they did not show vascular patterns different from that of HCC. Furthermore, the three cholangiocarcinoma did not present any delayed enhancement.

Nevertheless, our study has some limitations. Firstly, contrast-enhanced US, which is reported to significantly improve the accuracy of US for the evaluation of focal liver lesions [34, 35], was not included in this comparative study. This was because contrast-enhanced US is not routinely performed at our institution for this application due to difficulties in obtaining complete coverage of the liver during the dynamic vascular phases. Secondly, pathological confirmation of HCC was obtained for only 99 of 163 nodules (60.7 %). This was due to the small size of the nodules in some patients, and in other patients to the presence of multiple identically enhancing nodules, of which only one was biopsied. The 64 lesions without pathological confirmation were diagnosed as HCC based on identical enhancement features to other nodules in the same patient or because of a substantial increase in lesion size (>30 %) at follow-up MDCT or MRI. Thirdly, despite consensus reading being well accepted and commonly performed in research studies, it may not be as representative of actual practice as blinded reading.

A final limitation of the study is that no information was available regarding the presence of dysplastic nodules; these lesions are often problematical in the differential diagnosis with well-differentiated HCC [36, 37]

In summary, our study suggests that while US, MDCT and dynamic phase MRI may be appropriate for detection and characterisation of large (>2 cm) HCC nodules in patients with cirrhosis, significantly better sensitivity and diagnostic accuracy is achieved on dynamic + hepatobiliary phase MRI after the administration of gadobenate dimeglumine. A particular benefit of this latter technique may be in the evaluation of liver nodules between 1 and 2 cm in size, since the diagnostic performance achieved may obviate the need for lesion biopsy in certain patients with suspicious nodules.

References

1. Yang JD, Roberts LR (2010) Epidemiology and management of hepatocellular carcinoma. Infect Dis Clin North Am 24:899–919
2. Gomaa AI, Khan SA, Toledano MB, Waked I, Taylor-Robinson SD (2008) Hepatocellular carcinoma: epidemiology, risk factors and pathogenesis. World J Gastroenterol 14:4300–4308
3. Gambarin-Gelwan M, David CD, Shapiro R et al (2000) Sensitivity of commonly available screening test in detecting hepatocellular carcinoma in cirrhotic patients undergoing liver transplantation. Am J Gastroenterol 95:1535–1538
4. Reinhold C, Hammers L, Taylor CR et al (1995) Characterization of focal hepatic lesions with Duplex sonogrphy: findings in 198 patients. AJR Am J Roentgenol 164:1131–1135
5. Noguchi Y, Murakami T, Kim T et al (2003) Detection of hepatocellular carcinoma: comparison of dynamic MR imaging with dynamic double arterial phase helical CT. AJR Am J Roentgenol 180:455–460
6. Kim YK, Kim CS, Chung GH et al (2006) Comparison of gadobenate dimeglumine-enhanced MR and 16-MDCT for the detection of hepatocellular carcinoma. AJR Am J Roentgenol 186:149–157

7. Peterson MS, Baron RL, Marsh JW, Oliver JH III, Confer SR, Hunt LE (2000) Pretransplantation Surveillance for possible hepatocellular carcinoma in patients with cirrhosis: epidemiology and CT-based tumor detection rate in 430 cases with surgical pathologic correlation. Radiology 217:743–749
8. Sangiovanni A, Manini MA, Iavarone M et al (2010) The diagnostic and economic impact of contrast imaging techniques in the diagnosis of small hepatocellular carcinoma in cirrhosis. Gut 59:638–644
9. Teefey SA, Hildeboldt CC, Dehdashti F et al (2003) Detection of primary hepatic malignancy in liver transplant candidates: prospective comparison of CT, MR imaging, US, PET. Radiology 226:533–542
10. Libbrecht L, Bielen D, Verslype C et al (2002) Focal lesions in cirrhotic explant livers: pathological evaluation and accuracy of pretransplantation imaging examinations. Liver Transpl 8:749–761
11. Freeman RB, Mithoefer A, Ruthazer R et al (2006) Optimizing staging for hepatocellular carcinoma before liver transplantation: a retrospective analysis of the UNOS/OPTN database. Liver Transpl 12:1504–1511
12. Boone JM (2006) Multidetector CT: opportunities, challenges, and concerns associated with scanners with 64 or more detector rows. Radiology 241:334–337
13. Marin D, Catalano C, De Filippis G et al (2009) Detection of hepatocellular carcinoma in patients with cirrosi: added value of coronal multiplanar reformations from isotropix voxel with 64-MDCT. AJR Am J Roentgenol 192:775–782
14. D'Onofrio M, Faccioli N, Zamboni G et al (2008) Focal liver lesions in cirrohosis: value of contrast-enhanced ultrasonography compared with Doppler ultrasound and alpha-fetoprotein levels. Radiol Med 113:978–991
15. Baron RL, Oliver JH III, Confer S et al (1997) Screening cirrhosis for hepatocellular carcinoma (HCC) with helical contrast CT: specificity. Radiology 2005:143
16. Bruix J, Scherman M, Llovet JM et al (2001) Clinical managment of hepatocellular carcinoma. Conclusions of the barcellona-2000 EASL conference. Europe Assosation for the Study of the Liver. J Hepatol 35:421–430
17. Marin D, Di Martino M, Guerrisi A et al (2009) Hepatocellular carcinoma in patients with cirrhosis: qualitative comparison of gadobenate dimeglumine-enhanced MR imaging and multiphasic 64-section CT. Radiology 251:1–8
18. Kim JI, Lee MJ, Choi JY et al (2008) The value of gadobenate dimeglumine-enhanced delayed phase MR imaging for characterization of hepatocellular carcinoma nodules in the cirrhotic liver. Invest Radiol 43:202–210
19. Kim YK, Kim SC, Lee YH et al (2004) Comaprison of superparamgnetic Iron Oxide-Enhanced and gadobenate dimeglumine-enhanced MRI for detection of small hepatocellular carcinomas. AJR Am J Roentgenol 182:1217–1223
20. Hammerstingl R, Huppertz A, Breuer J et al (2008) Diagnostic efficacy of gadoxedic acid (Primovist)-enhanced MRI and spiral CT for a therapeutic strategy: comparison with intraopeartive and histological findings in focal lilver lesions. Eur Radiol 18:457–467
21. Di Martino M, Marin D, Guerrisi G et al (2010) Intraindividual comparison of gadoxetate disodium-enhanced MR imaging and 64-section multidetector CT in the detection of hepatocellular carcinoma in patients with cirrhosis. Radiology 256:806–816
22. Ebara M, Hatano R, Fukuda H et al (1998) Natural course of small hepatocellular carcinoma with underlying cirrhosis. A study of 30 patients. Hepatogastroenterology 45:1214–1220
23. International Working Party (1995) Terminology of nodular hepatocellular lesions. Hepatology 22:983–993
24. Harvey CJ, Albrecht T (2001) Ultrasound of focal liver lesions. Eur Radiol 11:1578–1593
25. Bruix J, Scherman M (2005) Management of hepatocellular carcinoma. Hepatology 42:1208–1236
26. Forner A, Vilana R, Ayuso C et al (2008) Diagnosis of hepatic nodules 20 mm or smaller in cirrhosis: prospective validation of non invasive diagnostic criteria for hepatocellular carcinoma. Hepatology 47:97–104
27. Chakraborty DP (2006) Analysis of location specific observer performance data: validated extensions of the jackknife free-response (JAFROC) method. Acad Radiol 13:1187–1193
28. Schwnke C, Busse R (2007) Analysis of differences in proportions from clustered data with multiple measurements in disgnostic studies. Methods Inf Med 46:548–552
29. Bruix J, Scherman M (2011) Management of hepatocellular carcinoma: an update. Hepatology 53:1020–1022
30. Vogl TJ, Stupavsky A, Pegios W et al (1997) Hepatocellular carcinoma: evaluation of dynamic and static gadobenate dimeglumine-enhanced MR imaging and histopatologic correlation. Radiology 205:721–728
31. Grazioli L, Morana G, Caudana R et al (2000) Hepatocellular Carcinoma: Correlation between gadobenate dimeglumine-enhanced MRI and pathologic findings. Invest Radiol 35:25–34
32. Morana G, Grazioli L, Kirchin MA et al (2011) Solid hypervascular liver lesions: accurate identification of true benign lesions on enhanced dynamic and hepatobiliary phase magnetic resonance imaging after gadobenate dimeglumine administration. Invest Radiol 46:225–239
33. Choi B, Kim T, Han J et al (2000) Vascularity of hepatocellular carcinoma: assessment with contrast-enhanced scond harmonic versus color Doppler ultrasound. Radiology 214:167–172
34. Strobel D, Kleinecke C, Hänsler J et al (2005) Contrast-enhanced sonography for the characterisation of hepatocellular carcinomas —correlation with histological differentiation. Ultraschall Med 26:270–276
35. Dănilă M, Sporea I, Sirli R, Popescu A, Sendroiu M, Martie A (2010) The role of contrast enhanced ultrasound (CEUS) in the assessment of liver nodules in patients with cirrhosis. Med Ultrason 12:145–149
36. Xu PJ, Yan FH, Wang JH, Shan Y, Ji Y, Chen CZ (2010) Contribution of diffusion-weighted magnetic resonance imaging in the characterization of hepatocellular carcinomas and dysplastic nodules in cirrhotic liver. J Comput Assist Tomogr 34:506–512
37. Bartolozzi C, Battaglia V, Bozzi E (2011) Hepatocellular nodules in liver cirrhosis: contrast enhanced MR. Abdom Imaging 36:290–299